Al-Nahrain Journal of Science
ANJS, Vol.28 (4), December, 2025, pp. 76-82

Study of Charge Density Distributions, Elastic and Inelastic Electron Scattering Form Factors and Size Radii for ^{24}Mg and ^{28}Si Nuclei

Zaid M. Abbas[1,2,*], Ghaith N. Flaiyh[1]

[1]Department of Physics, College of Science, University of Baghdad, Baghdad- Iraq
[2]Department of Medical Physics, College of Science, Al-Nahrain University, Baghdad- Iraq

Received: 03.02.2025
Accepted: 15.11.2025
Published: 15.12.2025

Keywords:
Unitary Correlation Operator Method,
Charge density distribution,
Elastic and Inelastic Form Factor

Abstract

Unitary Correlation Operator Method (UCOM) has been used to inspect the ground state properties of ^{24}Mg and ^{28}Si nuclei, such as, charge densities, the root mean square (rms) radii and elastic electron scattering form factors. Inelastic longitudinal electron scattering form factors have been computed for iso scalar or transition ΔT=0 of the ($0^+0 \rightarrow 2_1^+0$) and ($0^+0 \rightarrow 4_1^+0$ transitions) for the 24Mg and 28Si nuclei. The results of the computations have been discussed, and a comparison of those results with the experimental data has occurred. It was assured that the unitary correlation operator method is suitable for studying the nuclear structure.

http://doi.org/10.22401/ANJS.28.4.07

*Corresponding author: zaid.malk@nahrainuniv.edu.iq

1. Introduction

UCOM is a broad method that can be utilized to account for correlations in nuclear many-body systems that are caused by short-range interactions. The correlations can either be realized in effective operators defined by similarity transformations or imprinted in correlation-less many-body states like Slater determinants.UCOM is a limpid and axiomatic model since it directly presents correlation functions to describe short-range central and tensor correlations. States with several bodies are assigned a varying degree of freedom due to of these relationships [1]. When effective charges are utilized, one of the models that has been infallible in characterizing the static attributes of nuclei is the shell model within a limited model space. Form factor computations based solely on the model space wave function are insufficient to replicate electron scattering details. Consequently, it is necessary to incorporate core polarization effects into the computations [2]. Hamoudi et-al. examine the inelastic form factors, the shape of the ground state two body charge density distributions (2BCDD), the impact of the two body short-range correlation function and the Tassie model were all taken into consideration while evaluating the core polarization transition density in their work [3]. Roth et-al. provided a summary of advances in nuclear structure theory aimed at unitary transformation-based descriptions of these interaction-induced correlations [4]. They concentrated on UCOM, which provides a simple, all-encompassing, and reliable method for the handling of short-range correlations. They went into great detail on the UCOM formalism and emphasized how it relates to other approaches for describing short-range correlations and creating efficient interactions. Mahmood and Flaiyh have employed an effective two-body density operator [5]. For a point nucleon system with tensor force correlations. The operator has been utilized to derive a shape for the ground-state 2BCDD, which is viable in some light nuclei. The goal of the research is to examine the influences of central and tensor correlations on the ground state 2BCDD, root mean square charge radii, and elastic and inelastic scattering form factors for ^{24}Mg and ^{28}Si nuclei.

2. Theoretical formulations

The operator is utilized to express the nuclear density composed of A points, such as particles [6]:

$$\hat{\rho}^{(1)}\left(\vec{r}\right) = \sum_{i=1}^{A} \delta\left(\vec{r} - \vec{r}_i\right) \quad \ldots(1)$$

To convert this operator into a two-body density takes the shape of:

$$\sum_{i=1}^{A} \boldsymbol{\delta}(\vec{r}-\vec{r}_i) \equiv \frac{1}{2(A-1)} \sum_{i\neq j} \left\{ \boldsymbol{\delta}\left(\vec{r}-\vec{r}_i\right) + \boldsymbol{\delta}\left(\vec{r}-\vec{r}_j\right) \right\} \quad \dots(2)$$

Actually, the coordinates of the two particles, $\vec{r}_i$ and $\vec{r}_j$ can really undergo a beneficial transformation that is in express of relative ($\vec{r_{ij}}$) and center of mass ($\vec{R}_{ij}$) coordinates [7]:

$$\vec{r}_i = \frac{1}{\sqrt{2}}\left(\vec{R_{ij}} + \vec{r_{ij}}\right) \quad \dots(3-a)$$

$$\vec{r}_j = \frac{1}{\sqrt{2}}\left(\vec{R_{ij}} - \vec{r_{ij}}\right) \quad \dots(3-b)$$

Inserting equations (3-a) and (3-b) into eq. (2) get:

$$\hat{\rho}(2)\ \left(\vec{r}\right) = \frac{1}{2(A-1)} \sum_{i\neq j} \left\{ \delta\left[\vec{r} - \frac{1}{\sqrt{2}}\left(\vec{R}_{ij} + \vec{r}_{ij}\right)\right] + \delta\left[\vec{r} - \frac{1}{\sqrt{2}}\left(\vec{R}_{ij} - \vec{r}_{ij}\right)\right] \right\} \quad \dots(4)$$

Using the identity;

$$\delta(a\vec{r}) = \frac{1}{|a|}\delta(\vec{r})$$

Where a is a constant, then equation. (4) becomes:

$$\hat{\rho}(2)_{ch}\left(\vec{r}\right) = \frac{\sqrt{2}}{2(A-1)} \sum_{i\neq j} \left\{ \delta\left[\sqrt{2}\vec{r} - \vec{R}_{ij} - \vec{r}_{ij}\right] + \delta\left[\sqrt{2}\vec{r} - \vec{R}_{ij} + \vec{r}_{ij}\right] \right\} \quad \dots(5)$$

Two-body correlation functions $\tilde{C}$ can generate a correlated two-body charge density operator as follows:

$$\hat{\rho}(2)_{corr}\left(\vec{r}\right) = \frac{\sqrt{2}}{2(A-1)} \sum_{i\neq j} \tilde{C} \left\{ \delta\left[\sqrt{2}\vec{r} - \vec{R}_{ij} - \vec{r}_{ij}\right] + \delta\left[\sqrt{2}\vec{r} - \vec{R}_{ij} + \vec{r}_{ij}\right] \right\} \tilde{C} \quad \dots(6)$$

where the correlation operator C is described as [4,8]:

$$C = C_{\Omega} C_r \quad \dots(7)$$

where C_r central correlations and C_{Ω} describes tensor correlations, each of these unitary operators is indicated by [8]:

$$C_r = exp\left[-i\sum_{i<j} g_{r,ij}\right] \quad and \quad C_{\Omega} = exp\left[-i\sum_{i<j} g_{\Omega,ij}\right] \quad \dots(8)$$

The specifics of the generators g_r and g_{Ω} will rely on the particular NN interaction under account [8]. The *generator* for the central correlation is expressed in a *hermitized* shape as follows:

$$g_r = \sum_{S,T} \frac{1}{2}[q_r s_{ST}(r) + s_{ST}(r) q_r] \Pi_{ST} \quad \dots(9)$$

Where Π_{ST} is the dropping operator unto a two-body *spin* S and *sospin* T. For a two-body system, the correlation function may be computed using a numerically the function $R_+(r)$. Thus, the parameters used are the numerically specified $R_+(r)$ by [4,8]:

$$R_+(r) = r + \alpha\left(\frac{r}{\beta}\right)^{\eta} exp\{-exp(\frac{r}{\beta})\} \quad \dots(10)$$

The parameter α is dominant the aggregate magnitude of the shift, β is the length scale, and η is determined the steepness around $r = 0$.

In a hermitized form, the complete generator for the tensor correlations is expressed as follows:

$$g_{\Omega} = \sum_{T} \vartheta_T(r)\ S_{12}(\vec{r}\ , \vec{q}_{\Omega}) \Pi_{1T} \quad \dots(11)$$

Making use of the public definition for a rank 2 tensor operator:

$$S_{12}(\vec{a}\ , \vec{b}) = \frac{3}{2}\left[(\vec{\sigma}_1.\vec{a})(\vec{\sigma}_2.\vec{b}) + (\vec{\sigma}_1.\vec{b})(\vec{\sigma}_2.\vec{a})\right] - \frac{1}{2}\ (\vec{\sigma}_1.\vec{\sigma}_2)(\vec{a}.\vec{b} + \vec{b}\ .\vec{a}) \quad \dots(12)$$

The amplitude is presented by the tensor correlation function $\vartheta_T(r)$. For $\vartheta_T(r)$

The next parameter used is utilized [4,8]:

$$\vartheta_{(r)} = \alpha\ \left[1 - exp\left(-\frac{r}{\gamma}\right)\right] exp\left(-exp\left(\frac{r}{\beta}\right)\right) \quad \dots(13)$$

The expectation values of the associated two-body charge density operator of equation (6) provide the 2BCDD of nuclei, which can be written as follows:

$$\rho_{ch}(r) = \langle \Psi \mid \hat{\rho}(2)_{corr.}\left(\vec{r}\right) \mid \Psi \rangle = \sum_{i\langle j} \langle i\ j \mid \hat{\rho}(2)_{corr.}\left(\vec{r}\right)\ [\ \mid ij\ \rangle - \mid ji\ \rangle\ ] \quad \dots(14)$$

where two particles wave function is utilized by [9]:

$$[ij\rangle = \sum_{JM_J} \sum_{TM_T} \left\langle j_i m_i j_j m_j \middle| t_i m_t t_j m_{t_j} \right\rangle \left(j_i j_j\right) JM_J\rangle\ \left(t_i t_j\right) TM_T\rangle \quad \dots(15)$$

The space-spin portion $\left(j_i j_j\right) JM_J\rangle$ of the two-particle wave function built in the jj-coupling planner should be converted to the $\vec{r_{ij}}$ and $\vec{R}_{ij}$ coordinates since our correlated operator for the two-body charge density in equation (6) is created in these coordinates defines the mean square charge radii of the nuclei under consideration by [6].

$$\langle r^2 \rangle = \frac{4\pi}{Z} \int_0^{\infty} \rho_{ch}(r)\ r^4\ dr \quad \dots(16)$$

Utilizing the ground-state charge density allocation (from equation (14)), the elastic form factor should be examined. Since the fallen and dispersed electron waves are regarded as a plane wave, the form factor

in the Plane Wave Born Approximation is just the Fourier's convert of the CDD. As a result [10, 11]:

$$F(q) = \frac{4\pi}{Z}\int_0^\infty \rho_{ch}(r)\, j_0(qr) r^2 dr \quad \dots(17)$$

where $j_0(qr) = sin(qr)\frac{}{(qr)}$, equation (17) should be written as follows:

$$F(q) = \frac{4\pi}{qZ}\int_0^\infty \rho_{ch}(r)\, sin(qr) r \quad dr \quad \dots(18)$$

where $F_{fs}(q)$ is the adjustment for finite nucleon size and $F_{cm}(q)$ is the center of mass correction, our computations require multiplying the form factor of equation. (18) by these corrections; these take the forms [12].

$$F_{fs}(q) = e^{\frac{-0.43q^2}{4}} \quad \dots(19)$$

$$F_{cm}(q) = e^{\frac{q^2b^2}{4A}} \quad \dots(20)$$

Inserting these adjustments into equation. (18), we get;

$$F(q) = \frac{4\pi}{qZ}\int_0^\infty \rho_{ch}(r)\, Sin(qr) r \quad dr F_{fs}(q) F_{cm}(q) \quad \dots(21)$$

Inelastic longitudinal form factors, including angular momentum $J$and q, is given as follows [13].

$$\left|F_J^L(q)\right|^2 = \frac{4\pi}{Z^2(2J_i+1)}\left|\left\langle f\left\|\hat{T}_J^L(q)\right\|i\right\rangle\right|^2 \left|F_{cm}(q)\right|^2 \left|F_{fs}(q)\right|^2 \quad \dots(22)$$

The longitudinal operator is acquainted as [12]:

$$\hat{T}_{Jt_z}^L(q) = \int dr\; j_J(qr)\, Y_J(\Omega)\;\; \rho(r,t_z) \quad \dots(23)$$

where $\rho(r,t_z)$ is the operator of charge density. With the configuration mixing, the reduced matrix elements in *spin* and *isospin* space of the $\hat{T}_{Jt_z}^L(q)$ between the system's initial and final particle states are expressed as [12]:

$$\left\langle f \;\left\|\left|\hat{T}_{JT}^L\right|\right\| \; i\right\rangle = \sum_{a,b} OBDM^{JT}(i,f,J,a,b)\;\left\langle b \;\left\|\left|\hat{T}_{JT}^L\right|\right\| \; a\right\rangle \quad \dots(24)$$

OBDM is the One Body Density Matrix element, which is computed in formulas of the iso spin–reduced matrix element. The longitudinal operator of several particles reduced matrix elements is given as [12]:

$$\left\langle f\right\| \hat{T}_J^L(\tau_Z,q)\left\|i\right\rangle = \left\langle f\left\|\hat{T}_J^{ms}(\tau_Z,q)\right\|i\right\rangle + \left\langle f\left\|\hat{T}_J^{cor}(\tau_Z,q)\right\|i\right\rangle \quad \dots(25)$$

Equation (25) provides the model space matrix element as follows:

$$\left\langle f\left\|\hat{T}_J^{ms}(\tau_Z,q)\right\|i\right\rangle = e_i\int_0^\infty drr^2 j_J(qr)\,{}^{ms}\rho_{J,\tau_Z}(i,f,r) \quad \dots(26)$$

The model space transition density ${}^{ms}\rho_J(i,f,r)$ is given by [12]:

$$\rho_{J,\tau_z}^{ms}(i,f,r) = (i,f,J,j,j',\tau_z)\left\langle j\right\|Y_J\left\|j'\right\rangle R_{nl}(r)R_{n'l'}(r) \quad \dots(27)$$

The core- polarization matrix element in equation (25) take the ensuing shape [10, 11].

$$\left\langle f\left\|\hat{T}_J^{core}(\tau_Z,q)\right\|i\right\rangle = e_i\int_0^\infty drr^2 j_J(qr)\,{}^{core}\rho \quad (i,f,r) \quad \dots(28)$$

where ${}^{core}\rho_J$ is the core-polarization transition density (CP). So the overall transition density is:

$$\rho_{J\tau_z}(i,f,r) = (i,f,r) \quad \dots(29)$$

The CP is written by *Tassie* shape [14].

$$\rho_{Jt_z}^{core}(i,f,r) = N\frac{1}{2}(1+\tau_z)r^{J-1}\frac{d\rho_o(i,f,r)}{dr} \quad \dots(30)$$

where ρ_o is the ground state 2BCDD and N is a proportional constant is provided as [14]:

$$N = \frac{\int_0^\infty drr^{J+2}\,\rho^{ms}J\tau_z(i,f,r) - \sqrt{(2J_i+1)B(CJ)}}{(2J+1)\int_0^\infty drr^{2J}\rho_o(i,f,r)} \quad \dots(31)$$

where B(CJ) is the reduced transition probability.

3. Results and Discussion

The computations for the ground state 2BCDD's ($\rho_{ch}(r)$), the root mean square charge radii $\langle {r_{ch}}^2\rangle^{\frac{1}{2}}$, elastic and inelastic form factors $F(q)'s$ are examined for ^{24}Mg and ^{28}Si nuclei. The occupation probabilities of higher state is presented in Table (1). The force of the correlations are specified by suitable the computed $\langle {r_{ch}}^2\rangle^{\frac{1}{2}}$ with those of empirical data. All short-range and tensor parameters required in the computations of $\langle {r_{ch}}^2\rangle^{\frac{1}{2}}$, $\rho_{ch}(r)$ and $F(q)'s$ are presented in Table (1) and Table (2). Besides, the computed $\langle {r_{ch}}^2\rangle^{\frac{1}{2}}$ including the effect of UCOM are in good match with those of empirical data. Figure 1, illustrates the computed charge density distributions for ^{24}Mg (figure 1(a)) and ^{28}Si [figure 1(b)] nuclei got by UCOM parameters and without it, along with what fits into the empirical data (denoted by filled circle marks). We noticed that adding the influence of UCOM results to match the empirical data.

Table 1: Short-Range Central correlations Parameters which have been utilized in the current work's computations

Nuclei	Occupation percentage		$b\ (fm)$	$\alpha\ (fm)$	$\beta\ (fm)$	η	$\langle {r_{ch}}^2 \rangle^{\frac{1}{2}}$ (fm)	$\langle {r_{ch}}^2 \rangle^{\frac{1}{2}}$ (fm) Exp. [15]
^{24}Mg	$1d_{\frac{5}{2}}$	0.508	1.947	1.69	1.93	0.060	3.058678	3.0570
	$2s_{\frac{1}{2}}$	0.475						
^{28}Si	$\mathbf{1}\boldsymbol{d}_{\frac{5}{2}}$	0.8166	1.96	1.86	2.10	0.005	3.195795	3.1224
	$\mathbf{2}\boldsymbol{s}_{\frac{1}{2}}$	0.55						

Table 2: Tensor correlations, the parameters utilized in the current work's computations

Channel	$\alpha\ (fm)$	$\beta\ (fm)$	γ
$even\ \ S=0, T=1$	1.81	1.07	0.67
$even\ S=1, T=0$	1.43	0.95	0.78
$odd\ \ S=0, T=0$	2.3	1.0	0.9
$odd\ \ S=1, T=1$			

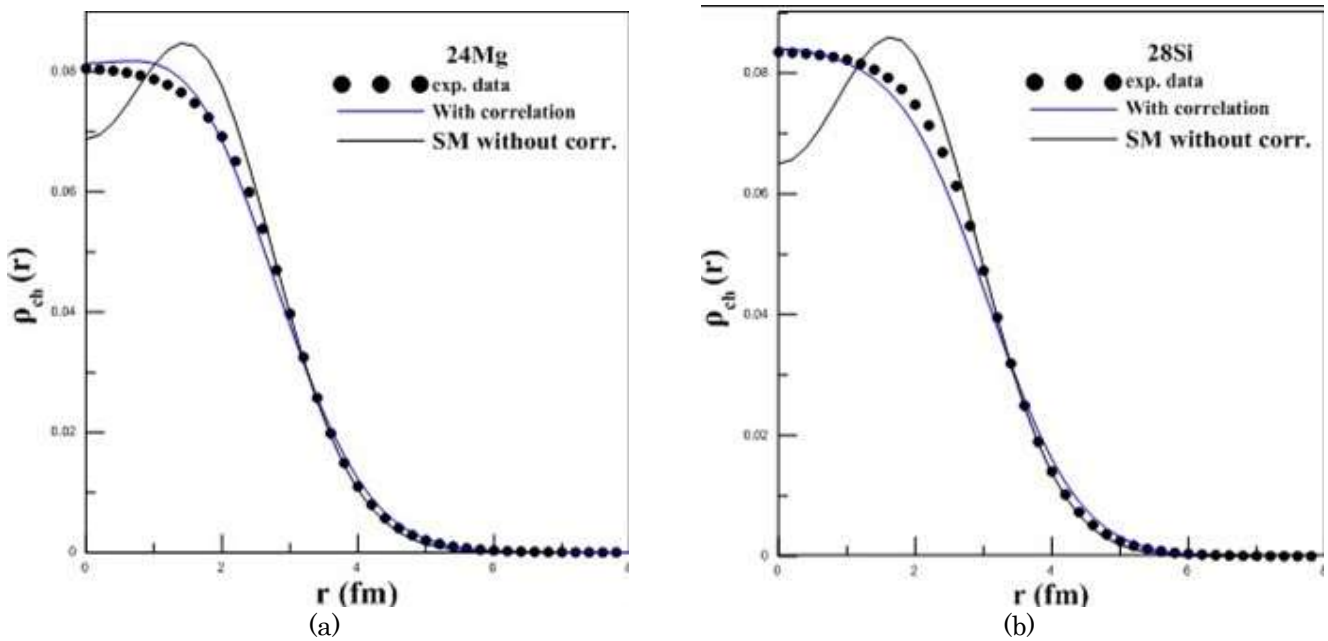

(a) (b)

Figure 1: Calculated charge density distribution for ^{24}Mg (Fig a) and ^{28}Si (Fig. b) nuclei with UCOM parameters with the exp. data [16]

The elastic form factors of ^{24}Mg and ^{28}Si nuclei are offered in figures (2.a) and (2.b), consecutively, it is noticeable from these forms that both the quantity and attitude of the computed form factors are in credible agreement with the empirical data during the entire zone of q. Moreover, the position of the computed diffraction minima in both computations of the curves is recreated in the true position. It is observed that the entrance of the UCOM in the computations of the red curve commands lightly enhanced outcomes of the computed form factors in the zone of q, and so tends to ameliorate the computed outcomes of form factors.

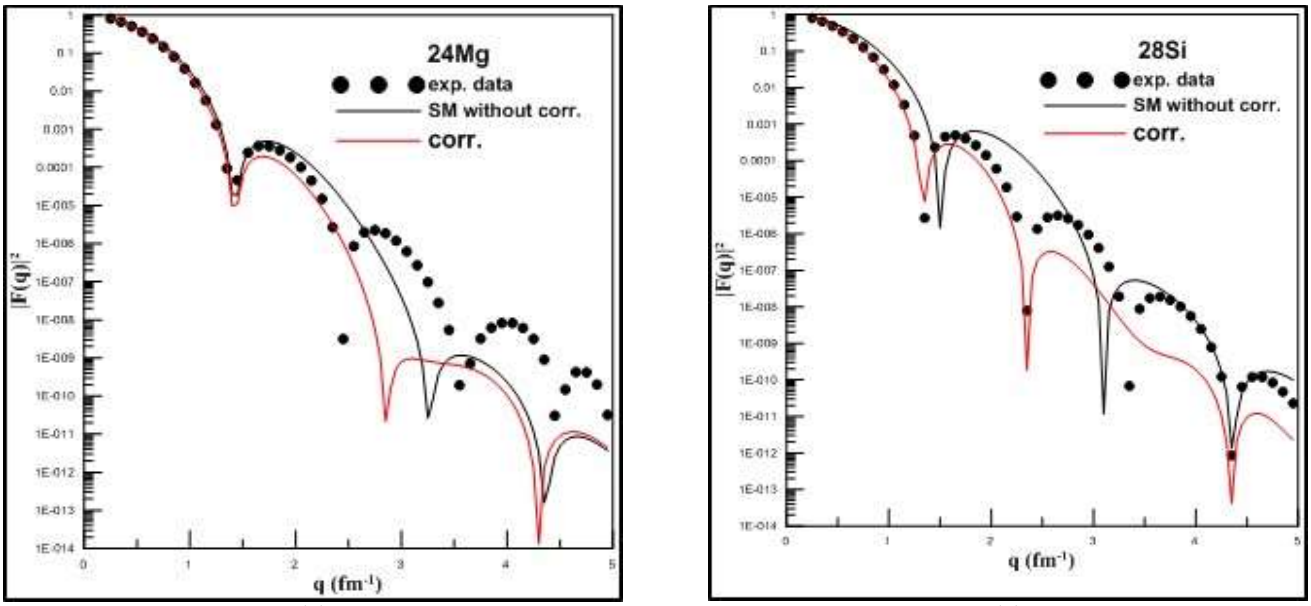

(a) (b)

Figure 2: Elastic Form Factor for ^{24}Mg (Fig. a) and ^{28}Si (Fig b) nuclei. The filled circle symbols are experimental data [16].

The inelastic longitudinal C2 form factors of ^{24}Mg and ^{28}Si nuclei are offered in figures 3(a) and 3(b) consecutively. The computed C2 form factors are schemed as a function of q for the transitions, $(J_i^\pi T_i \rightarrow J_f^\pi T_f)$,$0^+0 \rightarrow 2_1^+0$ (with an excitation energy of E_x=1.37 MeV [17] and $B(C2) = 404.7\, e^2.fm^4$ [18]) for ^{24}Mg and $0^+0 \rightarrow 2_1^+0$ (with E_x=1.78 MeV [19] and $B(C2) = 327.24 \pm 9.47 e^2.fm^4$ [20]) for ^{28}Si . In these shapes, red arches denote the contribution of the model space (MS) where the configuration mixing is regarded; blue curves denote the core polarization (CP) contribution where the influence of two-body correlations are regarded; black curves denote the total contribution, which is gained by taking MS together with CP influence into regard. We observe that adding CP into the MS enhances the results, ensuring better alignment with empirical details.

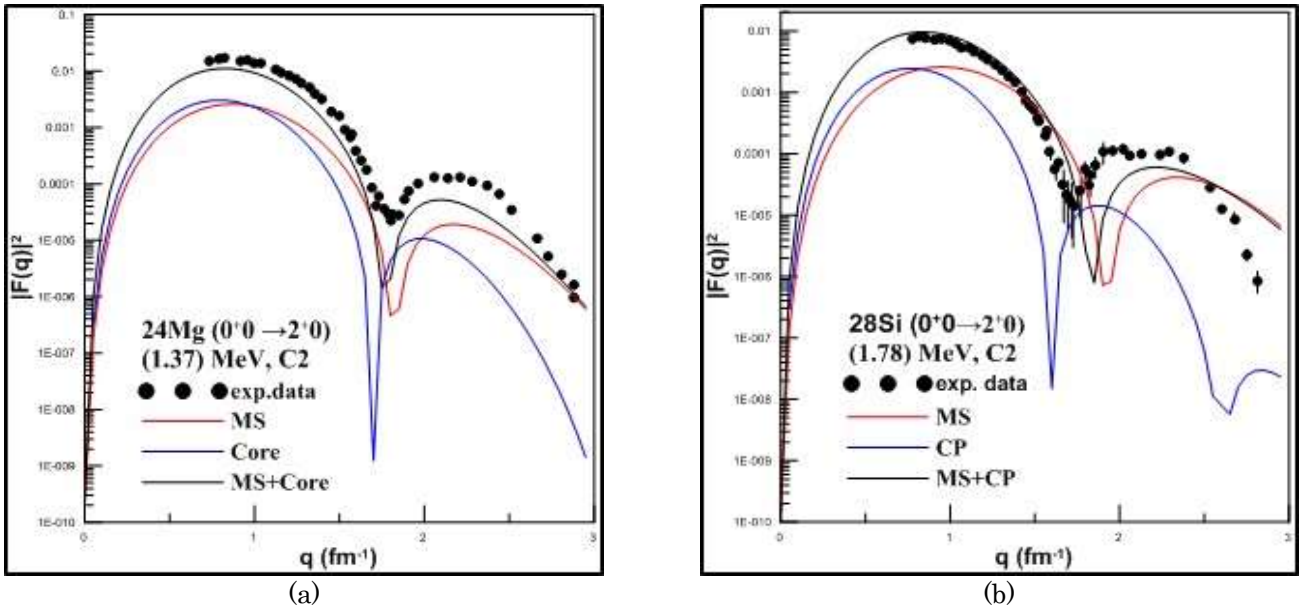

(a) (b)

Figure 3. The C2 form factors for ^{24}Mg (Fig. a) and ^{28}Si (Fig b) nuclei. The filled circle symbols are experimental data [18] and [19] respectively.

The inelastic longitudinal C4 form factors of ^{24}Mg and ^{28}Si nuclei are offered in figures 4(a) and 4(b), consecutively. The computed C4 form factors are schemed as a function of q for the transitions $0^+0 \rightarrow 4_2^+0$ in ^{24}Mg and $0^+0 \rightarrow 4_1^+0$ in ^{28}Si with excitation energies of $6.1\,MeV$ [20] and $4.617\,MeV$ [21] respectively. The $B(C4)$ of the above nuclei is $36000\,e^2.fm^4$ [20] and $27700\,e^2.fm^4$ [19] respectively. In these forms, red arches denote the contribution of MS where the configuration mixing is considered; blue arches denote CP contribution where the impact of two-body correlations are regarded, black arches denote the total contribution, which is gained by taking MS together with CP impacts into account. These figures clarify that MS is not able to offer a satisfying depiction comparable with empirical data for the zone of $q > 2\,fm^{-1}$ but merely CP influence inserted to MS, the gained outcomes for the longitudinal C4 form factors be reasonably in concurrence with those of empirical details during the entire zone of q as shown in the black arches of these figures.

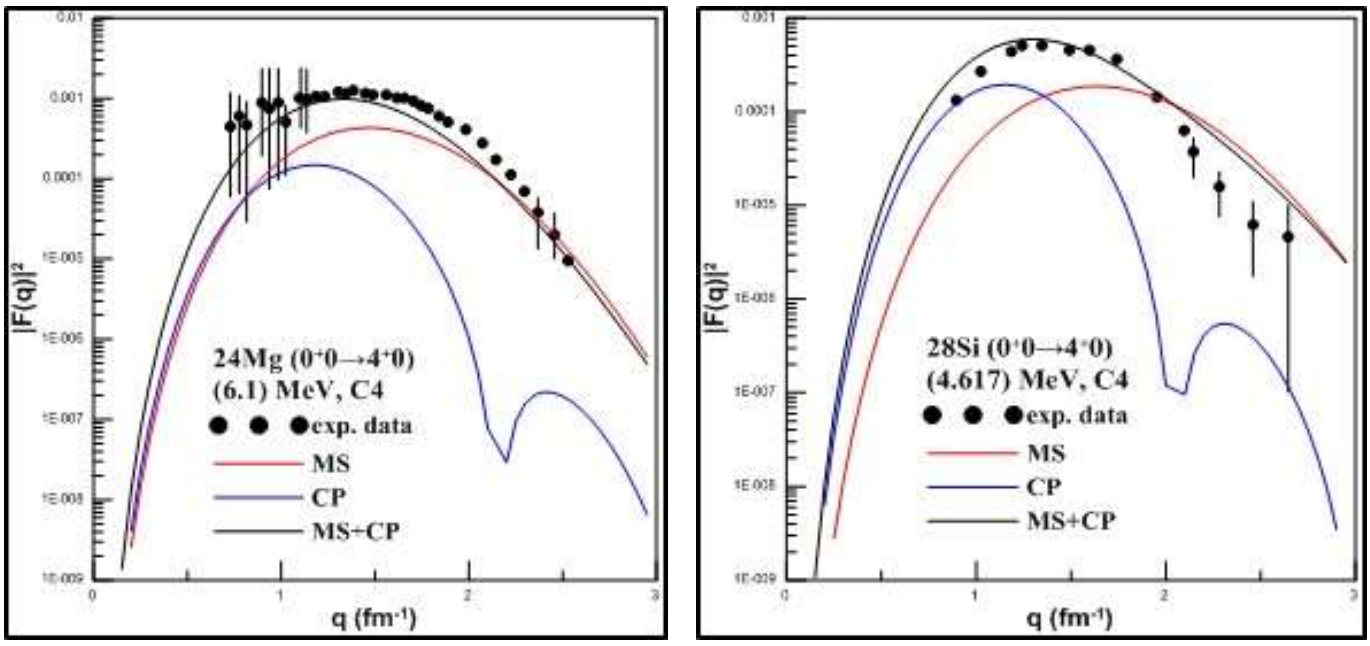

Figure 4: Inelastic longitudinal C4 form factors for ^{24}Mg (Fig. a) and ^{28}Si (Fig b) nuclei. The filled circle symbols are experimental data [19].

4. Conclusions

In the current work, by adding the UCOM to the 2BCDD's formula, we achieved an outstanding approval with the experimental outcomes for the $\rho_{ch}(r)$ and $\langle {r_{ch}}^2 \rangle^{\frac{1}{2}}$. Based on the $\rho_{ch}(r)$ using the elastic form factor calculations, we achieved a much with the experimental outcomes. In the computation of inelastic form factors, and based on the $\rho_{ch}(r)$ to account for the effect ofCP, we achieved results that match the experimental data. From the computed results of the form factor, we observed that adding CP to MS significantly improves the results, ensuring alignment with experimental values. Based on these findings, it is evident that utilizing the UCOM effect is highly effective in studying nuclear structure properties.

Conflicts of Interest: The authors declare no conflicts of interest.

Funding: No funds have been received for this work.

References

[1] Neff, T. and Feldmeier, H.; "Tensor correlations in the unitary correlation operator method", Nucl. Phys. A, 713 (3): 311-371, 2003.

[2] Flaiyh, G.N.; "Core Polarization Effects on the Inelastic Longitudinal Electron Scattering Form Factors of ^{48,50}Ti and ^{52,54}Cr nuclei", Iraqi J. Sci., 57 (1C): 639–650, 2016.

[3] Hamoudi, K.; Radhi, R.A.; Al-Taie, F.I.S. and Flaih, K.N.; "Calculation of the Inelastic Longitudinal Form Factors for Some Light Nuclei", J. Kerbala Univ., 7 (2): 117-130, 2009.

[4] Roth, R.; Neff, T. and Feldmeier, H.; " Nuclear structure in the framework of the Unitary Correlation Operator Method", Prog. Part. Nucl. Phys., 65(1): 50-93, 2010.
[5] Mahmood, L.A. and Flaiyh, G.N.; " Charge density distributions and electron scattering form factors of ^{19}F,^{22}Ne and ^{26}Mg nuclei", Iraqi J. Sci., 57 (3A): 1742-1747, 2016.
[6] Antonov, A.N.; Hodgson, P.E. and Petkov, I.Zh.; "Nucleon Momentum and Density Distribution in Nuclei". 1st ed.; Clarendon Press: Oxford, UK, 1988.
[7] Lawson, R.D.; "Theory of the Nuclear Shell Model". 1st ed.; Clarendon Press: Oxford, UK, 1980.
[8] Feldmeier, H.; Neff, T.; Roth, R. and Schnack, J.; " A unitary correlation operator method", Nucl. Phys. A, 632: 61–95, 1998.
[9] Heyde, K.L.G.; "The Nuclear Shell Model". 2nd ed.; Springer-Verlag: Berlin, Germany, 1994.
[10] Benson, H.G. and Flowers, B.H.; " A study of deformation in light nuclei: (II). Application to the even-parity states of the mass-18 nuclei", Nucl. Phys. A, 126: 332-354, 1969.
[11] Walecka, J.D.; "Electron Scattering for Nuclear and Nucleon Structure". 1st ed.; Cambridge University Press: Cambridge, UK, 2022.
[12] Brown, B.A.; Wildenthal, B.H.; Williamson, C.F.; Rad, F.N.; Kowalski, S.; Crannell, H. and O'Brien, J.T.; " Shell-model analysis of high-resolution data for elastic and inelastic electron scattering on ^{19}F", Phys. Rev. C, 32: 1127-1156, 1985.
[13] Radhi, R.A.; Alzubadi, A.A. and Manie, N.S.; " Electromagnetic multipoles of positive parity states in ^{27}Al by elastic and inelastic electron scattering", Nucl. Phys. A, 1015: 122302, 2021.
[14] Flaiyh, G.N.; " Inelastic electron scattering form factors involving the second excited 2+ level in the isotopes ^{50,54,52}Cr", Iraqi J. Phys., 13 (28): 19-26, 2015.
[15] Angeli, I. and Marinova, K.P.; " Table of experimental nuclear ground state charge radii: An update", At. Data Nucl. Data Tables, 99: 69–95, 2013.
[16] De Vries, H.; De Jager, C.W. and De Vries, C.; " Nuclear charge-density-distribution parameters from elastic electron scattering", At. Data Nucl. Tables, 36: 495–536, 1987.
[17] Yen, R.; Cardman, L.S.; Kalinsky, D.; Legg, J.R. and Bockelman, C.K.; " Determination of nuclear parameters by inelastic electron scattering at low-momentum transfer", Nucl. Phys. A, 235: 135, 1974.
[18] Hamoudi, A.K.; Radhi, R.A. and Flaiyh, G.N.; "Calculation of the longitudinal electron scattering form factors for the 2s-1d shell nuclei", Iraqi J. Phys., 9 (14): 47–56, 2011.
[19] Horikawa, Y.; Tovizuka, Y. and Nakada, A.; "Inelastic electron scattering form factors and hexadecapole transitions", Phys. Lett. B, 39: 9-15, 1971.
[20] Li, G.C.; Yearian, M.R. and Sick, I.; " High-momentum-transfer electron scattering from ^{24}Mg, ^{27}Al , ^{28}Si and 32S", Phys. Rev. C, 9: 1861-1877, 1974.
[21] Whitner, K.; Williamson, C.; Norum, B. E. and Kowalski, S.; " Inelastic electron scattering from ^{29}Si", Phys. Rev. C, 22: 374-383, 1980.